Final Draft
of the original manuscript:

Steinbrecht, S.; Koenig, R.; Schmidtke, K.-U.; Herzog, N.; Scheibner, K.; Krueger-Genge, A.; Jung, F.; Kammerer, S.; Kuepper, J.-H.:
Metabolic activity testing can underestimate acute drug cytotoxicity as revealed by HepG2 cell clones overexpressing cytochrome P450 2C19 and 3A4.
In: Toxicology. Vol. 412 (2019) 37 - 47.
First published online by Elsevier: November 27, 2018

DOI: /10.1016/j.tox.2018.11.008
https://dx.doi.org/10.1016/j.tox.2018.11.008

Metabolic activity testing can underestimate acute drug cytotoxicity as revealed by HepG2 cell clones overexpressing cytochrome P450 2C19 and 3A4

Susanne Steinbrecht[a], Rosalie König[a], Kai-Uwe Schmidtke[a], Natalie Herzog[a], Katrin Scheibner[a], Anne Krüger-Genge[b], Friedrich Jung[b], Sarah Kammerer[a] & Jan-Heiner Küpper[a]*.

[a] Institute of Biotechnology, Brandenburg University of Technology, Universitätsplatz 1, 01968 Senftenberg, Germany

[b] Institute of Biomaterial Science and Berlin-Brandenburg Center for Regenerative Therapies, Helmholtz-Zentrum Geesthacht, Kantstr. 55, 14513 Teltow, Germany

* Corresponding author, Email: jan-heiner.kuepper@b-tu.de, phone: +49 3573 85 930

Abstract

Preclinical drug safety assessment includes *in vitro* studies with physiological relevant cell cultures. As *in vitro* system for hepatic toxicology testing, we have been generating cell clones of human hepatoma cell line HepG2 by lentiviral transduction of phase I cytochrome P450 (CYP) enzymes. Here, we present a stable CYP2C19-overexpressing HepG2 cell clone (HepG2-2C19 C1) showing an enzyme activity of approximately 82 pmol x min^{-1} x mg^{-1} total cellular protein. The phenotypic stability over several passages of HepG2-2C19 C1 renders them to be a suitable reference cell clone for benchmarking CYP2C19 enzyme activity. In addition, we were interested to analyze acute cytotoxicity of cyclophosphamide metabolized by HepG2-2C19 C1 and by a previously generated CYP3A4-overexpressing HepG2 cell clone. Upon cyclophosphamide exposure, we were able to detect its metabolites 4-hydroxy-cyclophosphamide and acrolein in CYP3A4- and CYP2C19-expressing cell clones. XTT and ATP assays showed a modest reduction of cell viability of not more than 50 % with high dose (10 mM) CPA treatment. By contrast, dramatic acute cytotoxic effects of cyclophosphamide were evident by the formation of nuclear

γH2AX foci and by increased cell death events. These effects were by substantial decreases of cell membrane integrity as measured by trypan blue exclusion test.

Our data on CYP enzyme overexpressing HepG2 cell clones clearly show that cytotoxicity of CPA is dramatically underestimated by standard metabolic activity tests. Thus, additional tests to quantitate DNA damage formation and cell death induction might be required to realistically assess cytotoxicity of such compounds.

Keywords

Cyclophosphamide; cytochrome P450; hepatocyte; liver metabolism; toxicity, γH2AX foci

1. Introduction

Drug-induced liver injury (DILI) is the most frequent cause of drug failure during clinical testing and post market approval (Chan and Benet 2017). Thus, entry into clinical phases requires disclosure to regulatory authorities of substantial data from preclinical studies with animals and cell cultures to exclude acute and chronic drug toxicity effects. Therefore, many research groups attempt to establish *in vitro* liver cell culture systems to mimic cytochrome P450 (CYP450) metabolizing features (Castell et al. 2006; Gerets et al. 2012; Rueff et al. 1996; Yoshitomi et al. 2001). Liver biotransformation as a result of which many drugs become pharmacologically inactive decreases drug bioavailability. Furthermore, toxic drug metabolites can be produced. On the other hand, some prodrugs such as alkylating agent cyclophosphamide (CPA) are thought to be inactive *per se* and thus should require metabolic activation to exhibit their biological effects (Fleming 1997; Rodriguez-Antona and Ingelman-Sundberg 2006). CPA is widely used as an antitumor and immunosuppressive agent. Various human CYP450 enzymes such as CYP2A6, 2B6, 3A4/5, 2C9, 2C8, 2C18 and 2C19 were shown to perform monooxygenation of CPA leading to the phase I metabolite 4- hydroxyl-cyclophosphamide (4-OH-CPA) (Chang et al. 1997a; Chang et al. 1993; Chang et al. 1997b; Griskevicius et al. 2003; Ren et al. 1997; Rodriguez-Antona and

Ingelman-Sundberg 2006). 4-OH-CPA tautomerizes with aldophosphamide, which then can undergo *β*-elimination to generate the alkylating metabolite phosphoramide mustard (PM) and the toxic byproduct acrolein (Online Resource; Fig. S1) (Low et al. 1982; Sladek 1988). Since many years, *in vitro* studies on drug toxicity make use of complex hepatoma cell systems such as HepaRG (Aninat et al. 2006; Gerets et al. 2012; Guillouzo et al. 2007; Kanebratt and Andersson 2008; Lubberstedt et al. 2011) and more recently studies are also conducted on physiologically relevant non-transformed human hepatocytes. These cells are called Upcyte hepatocytes due to their feature of enhanced cell proliferation *in vitro* (Burkard et al. 2012; Herzog et al. 2016; Levy et al. 2015).

Due to their stable phenotype and simple cell culture conditions, numerous studies have been performed with human hepatoma cell line HepG2 (Ghallab 2014; Westerink and Schoonen 2007; Wilkening et al. 2003). These cells show many liver-specific functions, but their drawback is the lack functional expression of almost all relevant human liver phase I (CYP450) and phase II enzymes (Castell et al. 2006; Rodríguez-Antona et al. 2002).

To overcome the lack of CYP450 activity, we previously established HepG2 CYP3A4 clone 9 displaying activity of this enzyme at the upper range reported for primary human hepatocytes (Herzog et al. 2015). Here we present a new HepG2 cell clone stably overexpressing CYP2C19 (clone 1).

Acute cytotoxicity of chemicals and drugs is routinely evaluated by performing so called viability or metabolic activity tests based on reduction of tetrazolium dyes such as MTT, XTT or MTS, or on luminogenic ATP assays (Li et al. 2015; Riss et al. 2004; Sumantran 2011). There is increasing evidence that viability assays based on tetrazolium dyes can result in over- or underestimation of potential cytotoxicity effects (Stepanenko and Dmitrenko 2015; Vellonen et al. 2004; Wang et al. 2010). Based on the generation of HepG2 clones with stable overexpression of human CYP3A4 and CYP2C19, we were interested to re-evaluate acute cytotoxicity of cyclophosphamide as a prototype for cytostatic prodrugs.

2. Material and Methods

2.1 Cell culture and generation of CYP2C19-overexpressing HepG2 clones

Human hepatocellular carcinoma (HepG2) cells were (ATCC: HB-8065) were cultivated in Dulbecco's MEM growth medium (Biochrom AG, Berlin, Germany) supplemented with 10 % fetal bovine serum (Biochrom AG) and 2 mM L-Glutamine (PAA Laboratories GmbH, Pasching, Austria) at 37 °C and 5 % CO_2 in a humidified incubator. Medium for CYP2C19- and CYP3A4-overexpressing HepG2 clones was supplemented with 3 µg x ml^{-1} blasticidin (PAA, GE Healthcare, Austria). To generate CYP2C19-overexpressing HepG2 clones, human CYP2C19 cDNA (NCBI reference sequence: NM 000769) was cloned into lentiviral expression vector (Life Technologies GmbH, Darmstadt, Germany). Recombinant virus production and cell line generation were performed as described previously for CYP3A4-overexpressing cells (Herzog et al. 2015).

2.2 Determination of cell doubling times

4 x 10^4 cells/well were seeded into 6-well plates (Sarstedt SG & Co, Nümbrecht, Germany) and cultured under standard conditions. To determine cell doubling times, cells were counted every 1 or 2 days by using a Neubauer hemocytometer.

2.3 Western blot analysis

Larynx carcinoma cell line HEp-2 (ATCC:CCL-23), 293FT (Thermo Fisher Scientific, Waltham, USA; R70007), HepG2 and CYP-expressing HepG2 cell clones were harvested by trypsinization, pelleted, re-suspended in RIPA buffer (50 mM Tris, 150 mM NaCl, 0.5 % DOC, 1 % NP-40, 0.5 % SDS, 1 mM PMSF, pH 8) and incubated on ice for 15 min followed by centrifugation (10,000 x g, 10 min, 4 °C). Protein concentration of lysate supernatants were determined using Pierce™ BCA Protein Assay Kit (Thermo Fisher Scientific). Protein extracts and microsomes pooled from 50 different individual donors (Thermo Fisher Scientific) were mixed with Laemmli extraction buffer and heated at 95 °C for 5 min. 25 µg protein per lane were subjected to a 10 % SDS-PAGE and transferred to a Roti® PVDF

membrane (Carl Roth GmbH, Karlsruhe, Germany). After blocking, membranes were incubated with anti-CYP3A4 monoclonal (Biomol GmbH, Hamburg, Germany) or anti-CYP2C19 polyclonal antibody (St John´s Laboratory Ltd, London, UK), or anti-GAPDH monoclonal antibody (Antikörper-online GmbH, Aachen, Germany). After incubation with peroxidase-conjugated secondary antibodies (Sigma-Aldrich, St. Louis, USA), they were detected using a chemiluminescent system (ECL select, GE Healthcare, Freiburg, Germany) according to the manufacturer's instructions.

2.4 Reverse transcriptase-polymerase chain reaction (RT-PCR)

Cells (1-4 x 10^6) were harvested by trypsinization and pelleted. Total RNA was extracted using the innuPREP RNA Mini Kit (Analytik Jena AG, Jena, Germany) according to the manufacturer´s protocol. Total RNA was treated with *DNase I* (Thermo Fisher Scientific), and RNA integrity was controlled by 1 % agarose gel electrophoresis. Synthesis of cDNA was performed according to manufacturer´s protocol using oligo(dT)18 primer and RevertAid H Minus Reverse Transcriptase (both Thermo Fisher Scientific). The cDNA was used for PCR analysis of CYP2C19 (forward primer: 5`-TTGACCCTCGTCACTTTCTG-3`; reverse primer: 5`-GTTGTGTCAAGGTCCTTTGG-3`; BioTez, Berlin, Germany) and RPL-P0 (Ribosomal Protein Lateral Stalk Subunit P0; forward primer 5`-AAATGTTTCATTGTGGGAGC-3`; reverse primer 5`-ATATGAGGCAGCAGTTTCTC-3`; BioTez) using the Maxima Probe qPCR Master Mix (Thermo Fisher Scientific) and Evagreen (Biotium, Inc., Fremont, California, USA). PCR products were electrophoresed on a 3 % agarose gel.

2.5 Determination of enzyme activity

Cells (2 x 10^6 per well) were seeded into 6-well plates and further cultured for 3 days. Treatment with 250 µM of CYP2C19 substrate tolbutamide (Sigma-Aldrich) was performed in HepG2-medium lacking phenol red for 1 h in a humidified incubator at 5 % CO_2 and 37 °C. Tolbutamide conversion of 100 µg human liver microsomes (Thermo Fisher

Scientific) was performed by using 200 μM tolbutamide and 2 h of incubation. Supernatants were concentrated and prepared for HPLC and LC-MS by solid phase extraction using Strata™-X 33 μm Polymeric Reversed Phase (Phenomenex, Torrance, USA) according to manufacturer´s protocol. HPLC analysis of tolbutamide and 4-hydroxytolbutamide was accomplished with a VWR-Hitachi Elite LaChrom series HPLC (VWR International GmbH, Darmstadt, Germany) with photodiode array L-2455 (column: Phenomenex Kinetex C18, 4.6×150 mm, 5 μm particle size, 100 A°; security guard CK18, 4.6×2 mm). HPLC method: injection volume 20 μl; flow rate 1.0 ml x min^{-1}; column temperature 25 °C; mobile phase A (10 mM KH_2PO_4; pH 3); mobile phase B (acetonitrile); HPLC gradient profile: 0-5 min eluent B 5 %, 20 min eluent B 90 %, 25 min eluent B 90 %, 25.5 min eluent B 5 % and 30 min eluent B 5 %. Eluted substances were detected in the wavelength range 210–400 nm. LC-MS analysis was carried out on a Waters alliance HPLC system (2690 separation module; 2996 photo diode array detector) with a Mircomass ZMD single quadrupole mass spectrometer (Waters GmbH, Eschborn, Germany) ;ESI+; cone voltage: 30 V. Separation was on the same column as described for normal HPLC with mobile phase A (0.01 % formic acid) and B (acetonitrile). LC-MS method: injection volume 20 μl; flow rate 1.0 ml x min^{-1}; column temperature 25 °C; LC-MS gradient profile: 0-2 min eluent B 5 %, 22 min eluent B 90 %, 25 min eluent B 90 %, 25.5 min eluent B 5 % and 35 min eluent B 5 %. 4-hydroxytolbutamide was identified by comparison to an authentic standard (Sigma-Aldrich) based on retention time, UV absorption spectrum and mass spectrum $[M+H]^+$.

Quantification of 4-hydroxytolbutamide was carried out with calibration curves at corresponding λ = 230 nm. For determination of the enzyme activity related to total cellular protein, cells were harvested, lysed, and protein concentration was determined as described above.

2.6 Stability of substances

Stability of tolbutamide in ethanol and 4-hydroxytolbutamide in 50 % acetonitrile (200 μM) was investigated for samples kept at -20 °C (with and without two freeze-thaw cycles), room

temperature (RT; dark and with daylight), 4 °C and 37 °C for 24 h. Compounds were then analyzed by HPLC as described above. Stability of cyclophosphamide monohydrate (CPA) (Thermo Fisher Scientific) in H_2O (5 mM) was investigated for samples kept at -20 °C (with and without four freeze-thaw cycles), RT, 4 °C and 37 °C for three weeks. HPLC method: injection volume 20 µl; flow rate 1.0 ml x min^{-1}; column temperature 30 °C; mobile phase A (H_2O); mobile phase B (acetonitrile); HPLC gradient profile: 0-2 min B 5 %, 20 min B 50 %, 22 min B 50 %, 24 min B 5 % and 26 min B 5 %. Peaks were analyzed at a wavelength of 195 nm.

2.7 Cell treatment with cyclophosphamide

Cells were seeded in multi well plates (Sarstedt SG & Co, Nümbrecht, Germany) and cultured for 24 h. Following medium change, cells were exposed to different concentrations (0-10 mM) of CPA diluted in HepG2-medium as described above. After 24 h incubation, same volumes of CPA-containing HepG2 medium were added. After a total CPA exposure time of 48 h, medium was replaced by fresh HepG2-medium without CPA, and cells were further cultured for 72 h.

2.8 XTT and CellTiter-Glo®2.0 assay

Cells were seeded at a density of 1.5 x 10^4 cells/well in a 96-well plate and treated with CPA as described above. Cell viability was analyzed with the XTT assay (Cell Proliferation Kit II (XTT), Roche Diagnostics GmbH, Mannheim, Germany), according to the manufacturer´s protocol. The absorbance was measured after 6 h incubation time with the reaction mixture at a wavelength of 490 nm using a microplate reader (FLUOstar Omega, BMG Labtech, Ortenberg, Germany). CellTiter-Glo®2.0 assay (Promega, Madison; USA) was performed according to the manufacturer´s instructions.

2.9 Trypan blue exclusion assay

Cells were seeded at a density of 2 x 10^5 cells/well into 12-well plates and treated with CPA as described above. Cells were trypsinized and mixed with the same volume of trypan blue

(Amresco, Solon, USA). The fractions of viable cells, i.e. trypan blue-negative cells, were determined by using a Neubauer hemocytometer.

2.10 Detection of γH2AX foci

Cells (2.5 x 10^5) were seeded onto glass cover slips in 6-well plates (Carl Roth GmbH, Germany) and treated with CPA as described above. Then, cells were fixed in 4 % paraformaldehyde (Merck Millipore, Massachusetts, USA) for 10 min, washed with PBS and permeabilized in 0.25 % Triton X-100 (Carl Roth GmbH). Thereafter, cells were washed with PBS and incubated with anti-phospho-histone H2AX mouse monoclonal IgG (Merck Millipore). After washing, cells were incubated with polyclonal Cy3-conjugated goat-anti-mouse antibody (Jackson ImmunoResearch Laboratories, Inc., West Grove, USA) and 0.2 µg x ml^{-1} DAPI (Carl Roth GmbH). Immunofluorescence was evaluated with an Olympus IX81 fluorescence microscope (Olympus, Tokyo, Japan).

2.11 Flow cytometry

Cells (0.5-1 x 10^6) were seeded into 6-well plates and treated with CPA as described above. Thereafter, cells were harvested by trypsinization and centrifuged at 300 x g for 5 min. Cell pellets were re-suspended in 1 ml PBS per 1 x 10^6 cells and fixed with 4.5 ml of ice-cold 70 % (v/v) ethanol. After incubation for at least 1 h at 4 °C, cells were centrifuged twice at 300 x g for 5 min and washed with 5 ml PBS. Cell pellets were dissolved in 1 ml DNA staining solution (10 µg x ml^{-1} propidium iodide (Sigma-Aldrich), 100 µg x ml^{-1} DNase-free RNAse A (Qiagen N.V., Hilden, Germany) and 0,1 % (v/v) Triton X-100 (Carl Roth GmbH) in PBS) followed by incubation for 30 min at RT in the dark. Cellular fluorescence of at least 50,000 cells/sample was measured (solid-state diode ex 488 nm, em 585/42 nm) by flow cytometer (BD FACSCanto™ II, BD Bioscience, San Jose, California, USA). Data analysis was performed by using BD FACSDiva™ software.

2.12 4-OH-CPA detection

Cells were cultured in 6-well plates (1.5 x 10^6 cells/well) for two days and treated with 1 ml Krebs-Henseleit buffer (KHB from Sigma-Aldrich; completed with 25 mM $NaHCO_3$, 2 mM $CaCl_2$ x $2H_2O$, 25 mM HEPES, pH 7.4) containing 10 mM CPA for 6 h at 37 °C. Supernatants were immediately mixed with 0.67 M semicarbazide hydrochloride (pH 7.4) (3/10, v/v) (Carl Roth GmbH) for derivatization. Procedure was continued as described (Belfayol et al. 1995). HPLC method: injection volume 40 µl; flow rate 0.8 ml x min^{-1}; column temperature 25 °C; mobile phase A (25 mM K_2HPO_4; pH6); mobile phase B (acetonitrile); isocratic elution with A : B (82 : 18). UV wavelength for analysis was 230 nm. LC-MS method: injection volume 20 µl; flow rate 1.0 ml x min^{-1}; column temperature 25 °C; mobile phase A (formic acid (0.01 %), mobile phase B (acetonitrile). LC-MS gradient profile: 0-2 min B 5 %, 20 min B 30 %, 22 min B 80 %, 25 min B 80 %, 25,1 min B 5 % and 35 min B 5 %. Enzymatically produced 4-OH-CPA was identified by comparison with ozonized and derivatized CPA (Hohorst et al. 1976) as reference standard.

2.13 Acrolein detection

Cells were cultured in 6-well plates (2 x 10^6 cells/well) for two days and treated with 500 µl KHB containing different concentrations (0-10 mM) of CPA for 6 h at 37 °C. 200 µl of supernatants were transferred to tubes containing 100 µl of 3-aminophenol (5 mg x ml^{-1}; Sigma-Aldrich) and hydroxylamine hydrochloride (6 mg x ml^{-1}; AppliChem GmbH, Darmstadt, Germany) in 3 N HCl. The mixture was incubated at 99 °C for 15 min, cooled to RT in the dark and transferred to a black 96-well plate. The absorbance of the product 7-hydroxyquinoline was measured by a microplate reader (FLUOstar Omega) with an excitation wavelength of 355 nm and an emission wavelength of 500 nm. Quantification of acrolein was carried out with a calibration curve using commercial acrolein (Sigma-Aldrich).

2.14 Statistical analysis

Statistical analyses were done using one-way ANOvA followed by Dunnett's multiple comparison test. All analyses were performed with GraphPad Prism 6.0 (GraphPad Software Inc., La Jolla, CA, USA). If not stated otherwise, at least three independent experiments were performed in every instance. Results were considered as statistically significant if $p<0.05$.

3. Results

3.1 Generation of HepG2 cell clones overexpressing human CYP2C19

To study effects of cyclophosphamide, we used a previously established HepG2 cell clone stably overexpressing CYP3A4 (Herzog et al. 2015) and generated a new clone overexpressing CYP2C19.

HepG2-3A4 C9 was shown to have a more than 10,000-fold increase in CYP3A4 mRNA levels as well as a stable CYP3A4 enzyme activity of about 600 pmol x min^{-1} x mg^{-1} total cellular protein measured by testosterone conversion (Herzog et al. 2015).

To also generate a CYP2C19 clone, HepG2 cells were transduced with human CYP2C19-encoding lentivirus followed by antibiotic selection and isolation of cell clones. For further analyses, we choose clone 1 from all clones tested because of its clear-cut CYP2C19 expression and enzyme activity (see below).

Clone 1 (C1) retained the cobblestone-like morphology and formation of cell agglomerates typical for parental cell line HepG2 (Fig. 1a). Moreover, cell doubling times did not differ significantly between HepG2-CYP2C19 C1 and parental HepG2 cells (Fig 1b). Novel HepG2 cell clone 2C19 C1 displayed clear RNA and protein overexpression of CYP2C19 (Fig. 1c, d). The previously generated clone HepG2-3A4 C9 (Herzog et al. 2015) as well as our newly established CYP2C19 clone displayed stable protein expression levels of their recombinant CYP enzymes over at least six passages (Fig. 1d, e). As expected, both CYP2C19 and CYP3A4 expression were below detection limit in parental HepG2 cells. Western Blot experiments revealed strong expression of CYP2C19 and CYP3A4 in the

respective HepG2 cell clones. Both proteins could also be detected in the positive control, i.e. commercially available human liver microsomes, which were pooled from 50 donors (Fig. 1d).

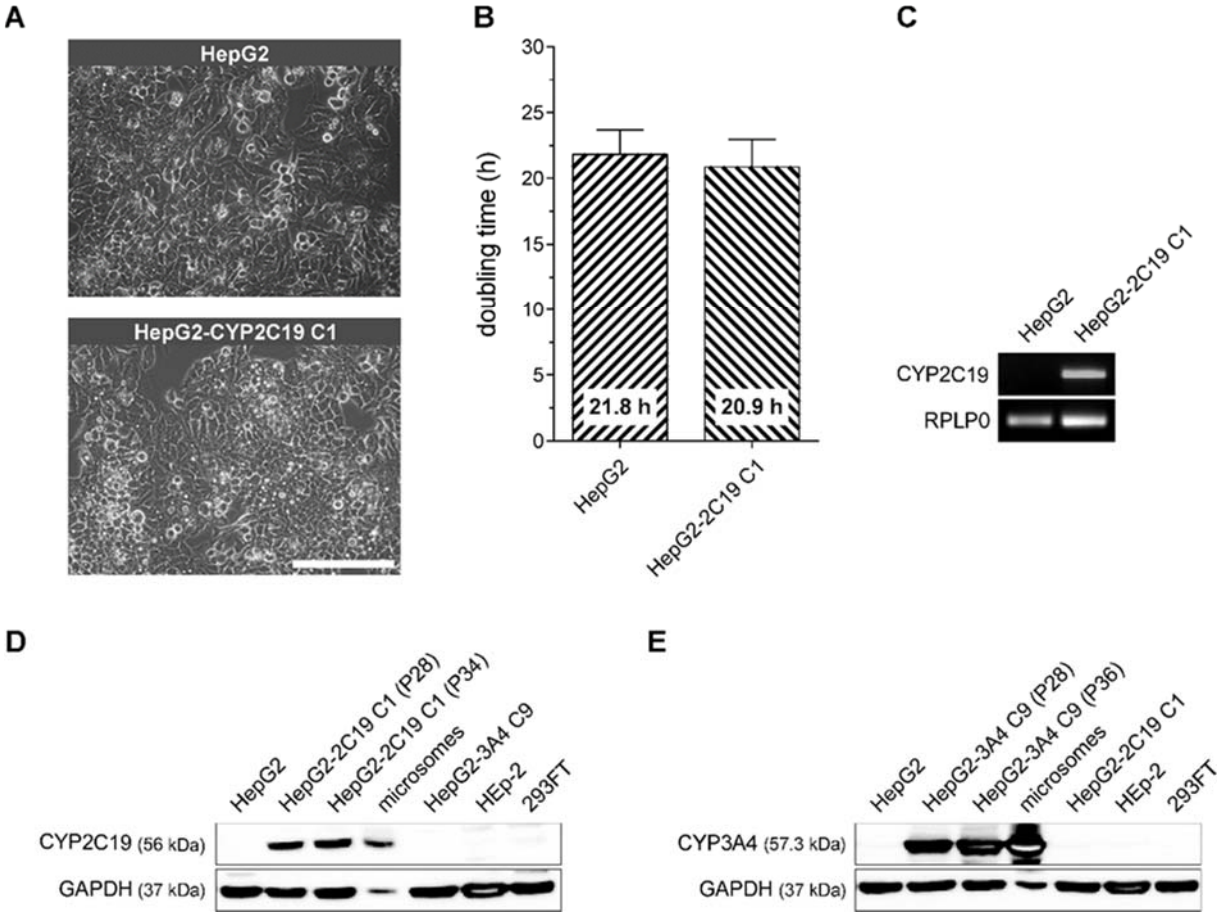

Fig. 1 Phenotypic characterization of HepG2-2C19 clone 1. (**a**) Phase contrast microscopy of HepG2-CYP2C19 C1 and parental cell line HepG2 cultivated as exponentially growing monolayers. Images were obtained with microscope CKX41 and 10x objective (scale bar 200 µm). (**b**) Cell doubling times of exponentially growing cultures of HepG2-2C19 C1 and HepG2. (**c**) Agarose gel electrophoresis of RT-PCR products of CYP2C19 gene expression in HepG2-2C19 C1 and HepG2. RPLP0 was used as reference gene. Western blot analysis of CYP2C19 (**d**) and CYP3A4 (**e**) expression in HepG2 cell clones and controls. Equal protein amounts (25 µg) of HepG2, HEp2, 293FT as well as HepG2-2C19 C1 and HepG2-3A4 C9 in different passages were used for Western blotting as indicated. HEp-2 and 293FT cells were used as negative controls, whereas 25 µg microsome protein served as positive control for CYP expression. GAPDH was used as protein loading control. Note that microsomal protein extracts do have relatively lower GAPDH protein levels than whole cell extracts.

For further phenotypic characterization**,** we tested the functionality of expressed CYP2C19 in HepG2-2C19 clone 1 compared to HepG2 cells and human liver microsomes. To measure CYP2C19 enzyme activity, first-generation diabetes type II drug tolbutamide was used as standard substrate. CYP2C19 is involved in metabolization of tolbutamide to form 4-hydroxytolbutamide (Lasker et al. 1998; Wester et al. 2000). We verified by HPLC

analysis that tolbutamide dissolved in ethanol and 4-hydroxytolbutamide dissolved in 50 % acetonitrile are stable at -20 °C (with and without two freeze-thaw cycles), at 4 °C, at room temperature (dark and with daylight) and at 37 °C for at least 24 h. This indicates that conversion and measurement of tolbutamide and its metabolite are unaffected by degradation procedures under cell culture conditions (37 °C). Using HepG2-2C19 C1 cells, we found that recombinant CYP2C19 expression led to a stable and reproducible enzyme activity of about 82 (± 18.82) pmol x min^{-1} x mg^{-1} total cellular protein over at least eight passages of this cell clone. Parental HepG2 cells did not show any HPLC-detectable formation of 4-hydroxytolbutamide. We compared the total cellular CYP2C19 activity of HepG2-2C19 C1 with that of pooled microsomes as positive control. Normalized to time and total protein amount, tested microsomal preparation displayed a tolbutamide hydroxylation activity of about 85 (± 10.12) pmol x min^{-1} x mg^{-1}.

3.2 Moderate effect of short-term cyclophosphamide exposure on metabolic activity of HepG2 cells and clones thereof

CYP2C19 and CYP3A4, among other CYP enzymes, are known to be involved in hydoxylation of CPA (Chang et al. 1993; Ren et al. 1997; Roy et al. 1999). Further reaction steps to form the active and toxic CPA metabolites acrolein and phosphoramide mustard (PM) are non-enzymatic.

To set up the experimental design for acute cytotoxicity testing of CPA, we first analyzed by HPLC the stability of CPA at different temperatures. CPA in water was stable at -20 °C (without and with four freeze-thaw cycles) and at 4 °C for three weeks. This indicates that CPA stock solutions can be stored both at -20 °C and at 4 °C for several weeks without loss of activity. By contrast, we found that CPA incubation at cell culture conditions, *i.e.* at 37 °C caused about 8 % decrease of CPA concentration in 24 hours.

We next exposed HepG2 cells and clones thereof to different CPA concentrations for up to 48 hours which is in line with acute cytotoxicity analysis. Because of the found CPA prodrug instability, cells were supplemented with fresh CPA-containing medium 24 hours after start

of experiment. In order to assess the effect of CPA on metabolic activity such as rate of glycolysis, we performed standard XTT and ATP assays. Figure 2a clearly shows that the optimized XTT assay we used did not reveal any significant decrease of metabolic activity with 5 mM CPA in all tested cell lines, and even high-dose CPA treatment showed only a moderate decrease, which is highest in CYP3A4-expressing cells. Figure 2b shows that when metabolic activity is determined by CellTiter-Glo®2.0 assay, which quantitates cellular ATP levels, CPA effects become more obvious, but still seem not to fully represent the acute cytotoxicity which can be expected in liver cells.

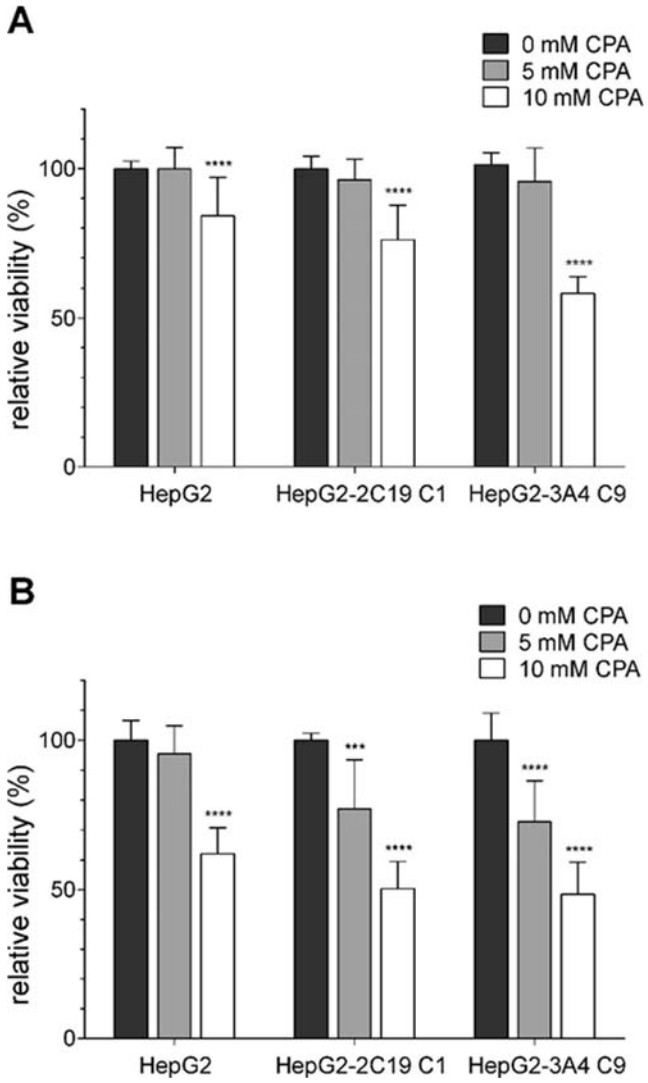

Fig. 2 Metabolic activity of CPA-treated HepG2 cell clones. Relative cell viability of HepG2 cell clones after CPA treatment was evaluated by (**a**) XTT (as absorbance (A_{490nm} – A_{655nm}) and (**b**) CellTiter-Glo®2.0 assay (as ATP levels). Data represent the mean ± SD and were compared to untreated controls; ***p<0.001; ****p<0.0001.

3.3 Acute cytotoxicity of cyclophosphamide is clearly evident from DNA damage formation and cell death induction

To compare CPA effects on metabolic activity with those on cell death induction, we next directly measured cell membrane integrity, DNA damage formation and cell death rates. Since CPA cytotoxicity is thought to be mediated by the production of toxic metabolites via CYP3A4 and CYP2C19, we first attempted to detect 4-OH-CPA, which is the first reaction product from liver biotransformation of CPA. Indeed, HPLC analyses revealed a clear peak of the expected semicarbazone derivative of 4-OH-CPA with a retention time of about 6 min at 230 nm for CPA-treated CYP-overexpressing HepG2 cell clones, which was absent in negative controls (HepG2 cells, HepG2 cell clones without CPA treatment; Supplementary material, Fig. S2). The mass spectrum of LC-MS showed a predominant protonated molecule at *m/z* 334 which is in line with the predicted molecular weight of the metabolite derivative (Belfayol et al. 1995). There was no such peak detectable if samples from negative controls were analyzed.

Phase I metabolite 4-OH-CPA is in equilibrium with the intermediate metabolite aldophosphamide which then gives rise to stoichiometrically equal amounts of cytotoxic compounds PM and acrolein (Supplementary material, Fig. S1). In contrast to PM, there is a convenient detection method available for acrolein. Figure 3 shows that acrolein formation is clearly detectable in CPA-treated CYP-overexpressing HepG2 cell clones, while this metabolite could not be detected in parental HepG2 cells.

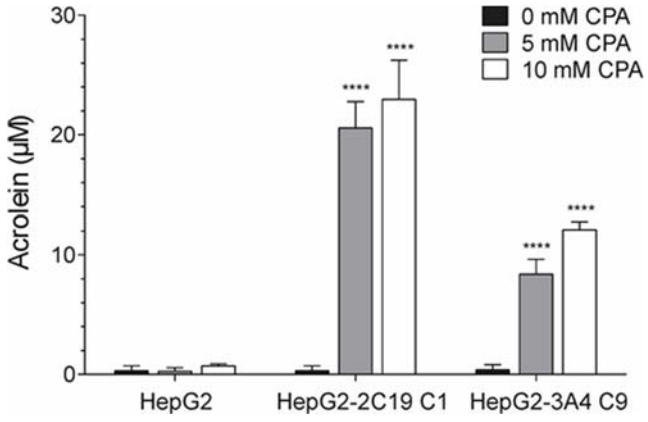

Fig. 3 Acrolein formation in CPA-treated HepG2 cell clones. Cells were exposed to the indicated concentrations of CPA for 6 h. Culture supernatants were used for derivatization of acrolein as

described in the materials and methods section. Quantified data represent the mean ± SD. ****p<0.0001

We next tested the biological effects of CPA exposure on cell death induction. As expected, 5-10 mM CPA caused a substantial decrease in cell culture confluency of novel HepG2 clone with CYP2C19 overexpression, which is clearly visible by microscopic examination. The same decrease of cell density was observed with HepG2 3A4 cells while HepG2 cells apparently were much less affected (Fig. 4a). In addition to microscopic examination of cytotoxicity, we analyzed the effect of CPA on cell membrane integrity by trypan blue exclusion test. As is apparent from Figure 4b, there were dramatic reductions in cell membrane integrity visible when our cell clones were treated with CPA, with stronger effects in HepG2 CYP3A4 cells than in CYP2C19 cells. Interestingly, we also observed a reduction of cell membrane integrity in CPA-treated HepG2 parental cells. Since we could not detect expression of CPA-metabolizing CYP enzymes CYP2C19 and 3A4 in HepG2 cells (Fig. 1d, e), observed toxicity could be due to some CPA-activating activity of CYP2B6. Expression levels of this enzyme were found to be about 1-10 % of that from pooled primary human hepatocytes while expression levels of other CPA-metabolizing enzymes were several orders of magnitude lower (Westerink and Schoonen 2007; Wilkening et al. 2003). Altogether, reductions in cell membrane integrity of CPA-treated cells were clearly stronger in CYP-overexpressing HepG2 cell clones than in parental cells.

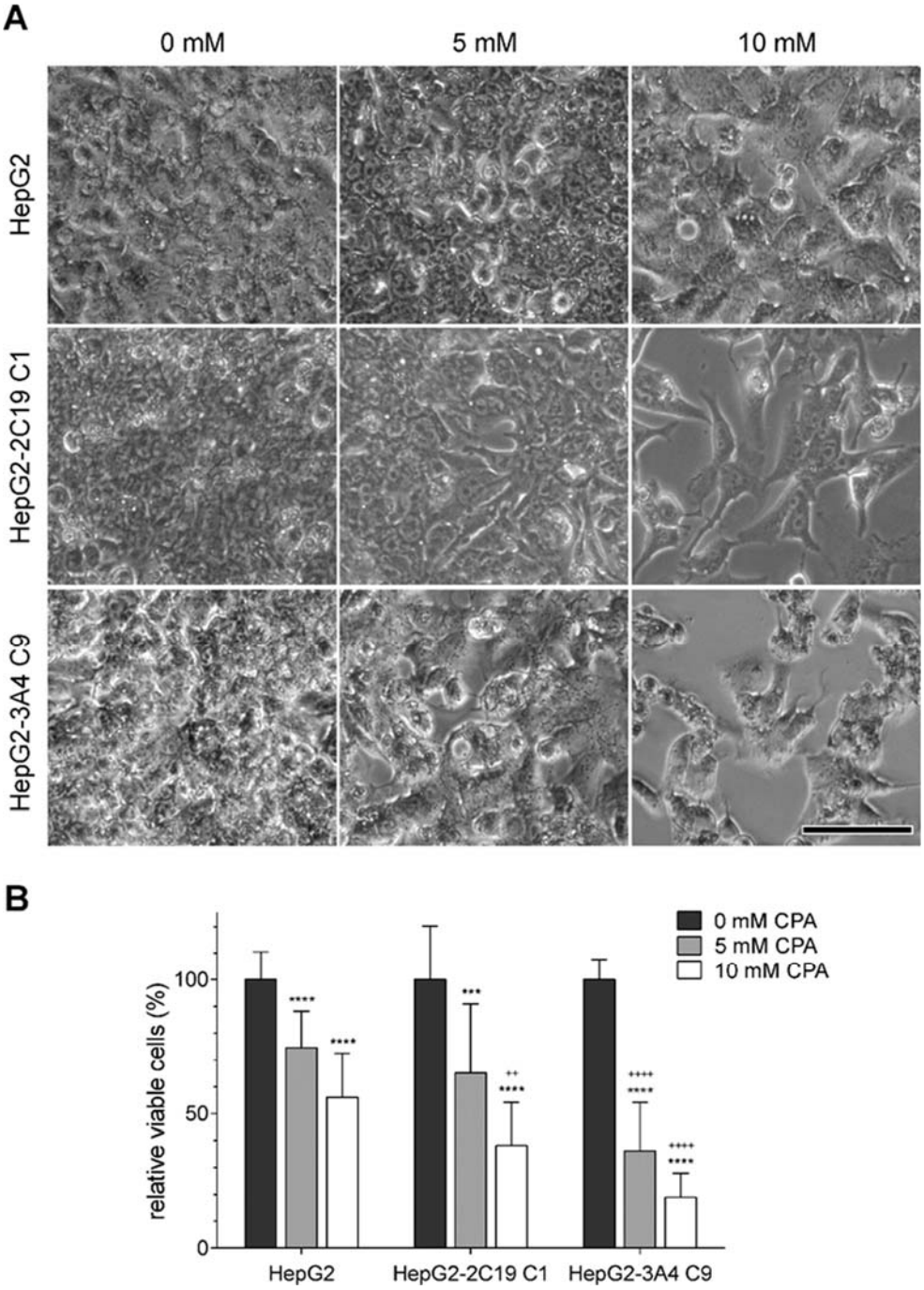

Fig. 4 Cell density and cell membrane integrity of CPA-treated HepG2 cells and cell clones. (**a**) Phase contrast images were obtained with microscope CKX41 and 10x objective (scale bar 100 µm). (**b**) Relative viability of cells was evaluated by trypan blue exclusion test. Data represent the mean ± SD of six independent experiments; data were expressed as relative number of trypan blue negative cells in % of treated cells compared to the respective control; * = comparison of different treatments within the same cell line, but untreated; ***p<0.001; ****p<0.0001; $^{+}$ = comparison of different cell lines with same CPA treatment; ^{++}p<0.01; ^{++++}p<0.0001.

To directly analyze expected genotoxicity of CPA, we investigated by indirect immunofluorescence the formation of γH2AX foci (Kuo and Yang 2008; Zhou et al. 2006)

as indicator for the known DNA-damaging activity of PM (Colvin et al. 1976; Crook et al. 1986). The induction of H2AX phosphorylation leading to γH2AX foci in nuclei of CYP-expressing HepG2 cell clones and HepG2 cells was measured following exposure to CPA concentrations up to 10 mM for 48 h. The nuclear regions of CYP-expressing HepG2 cell clones and HepG2 cells showed a clear increase in γH2AX formation with higher CPA concentrations used (Fig. 5; representative images of HepG2-2C19 C1 in Figure 5a). HepG2-2C19 C1 and HepG2-3A4 C9 apparently were more sensitive towards CPA genotoxicity than parental HepG2 cells. Exposing cells with 5 mM CPA caused 3-4 times more nuclei with > 50 γH2AX foci in CYP-overexpressing cell clones than in parental HepG2 cells (Fig. 5b). Altogether, HepG2 clones which were treated with 5 or 10 mM CPA showed a higher than 50-fold increase of nuclei containing accumulated γH2AX foci compared to non-treated cells. These dramatic difference between CPA-treated and untreated cells are in marked contrast to only moderate effects which were visible upon analyses of metabolic activities (Fig. 2).

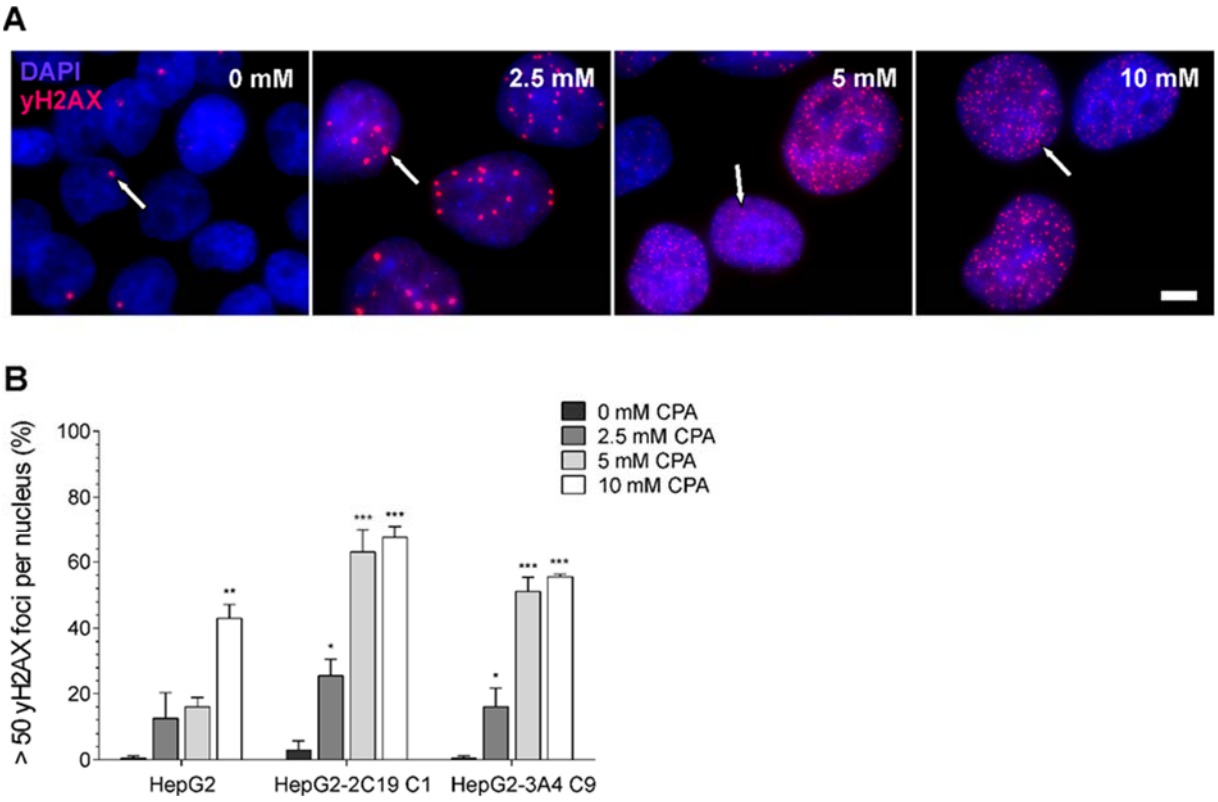

Fig. 5 Genotoxicity of CPA on CYP-overexpressing HepG2 cell clones and HepG2. Immunofluorescence for visualization of γH2AX was performed as described in the materials and

methods section. (**a**) Representative images of a γH2AX-specific immunofluorescence on HepG2-CYP2C19 C1 cells treated or not with CPA as indicated. Nuclei were stained with DAPI. Images were obtained with Olympus IX81 fluorescence microscope and 100x objective (scale bar 5 µm). (**b**) Quantification of γH2AX foci per nucleus as percentages of nuclei with more than 50 γH2AX foci. Data represent the mean ± SD from two separate experiments; **p*<0.05; ***p*<0.01; ****p*<0.001.

In order to investigate how CPA affects the biological endpoint of cell death induction in HepG2 cells and cell clones, we performed flow cytometry analyses. Figure 6a shows for CYP2C19-overexpressing HepG2 cells that 5 mM CPA treatment resulted in a substantial decrease of G0/G1 cells and an apparent accumulation of cells in S-phase. Similar results were reported previously to occur after CPA and nitrogen mustard treatment of cells (Cai et al. 2001; Chernoff et al. 1989; Dean and Fox 1984). After 10 mM CPA treatment, we found a dramatic increase of sub-G_1 events, which is indicative for apoptosis (Beneke et al. 2000; Darzynkiewicz et al. 2010; Plesca et al. 2008). Quantification of sub-G_1 cells after 10 mM CPA exposure revealed that HepG2 cells showed moderate CPA-induced apoptosis, while HepG2 cell clones with CYP overexpression showed substantial increases of cell death induction (Fig. 6b). The relatively high percentage of “background” subG1 events in CPA-untreated cells might be due to the fact that those cultures reached confluency during the experiment.

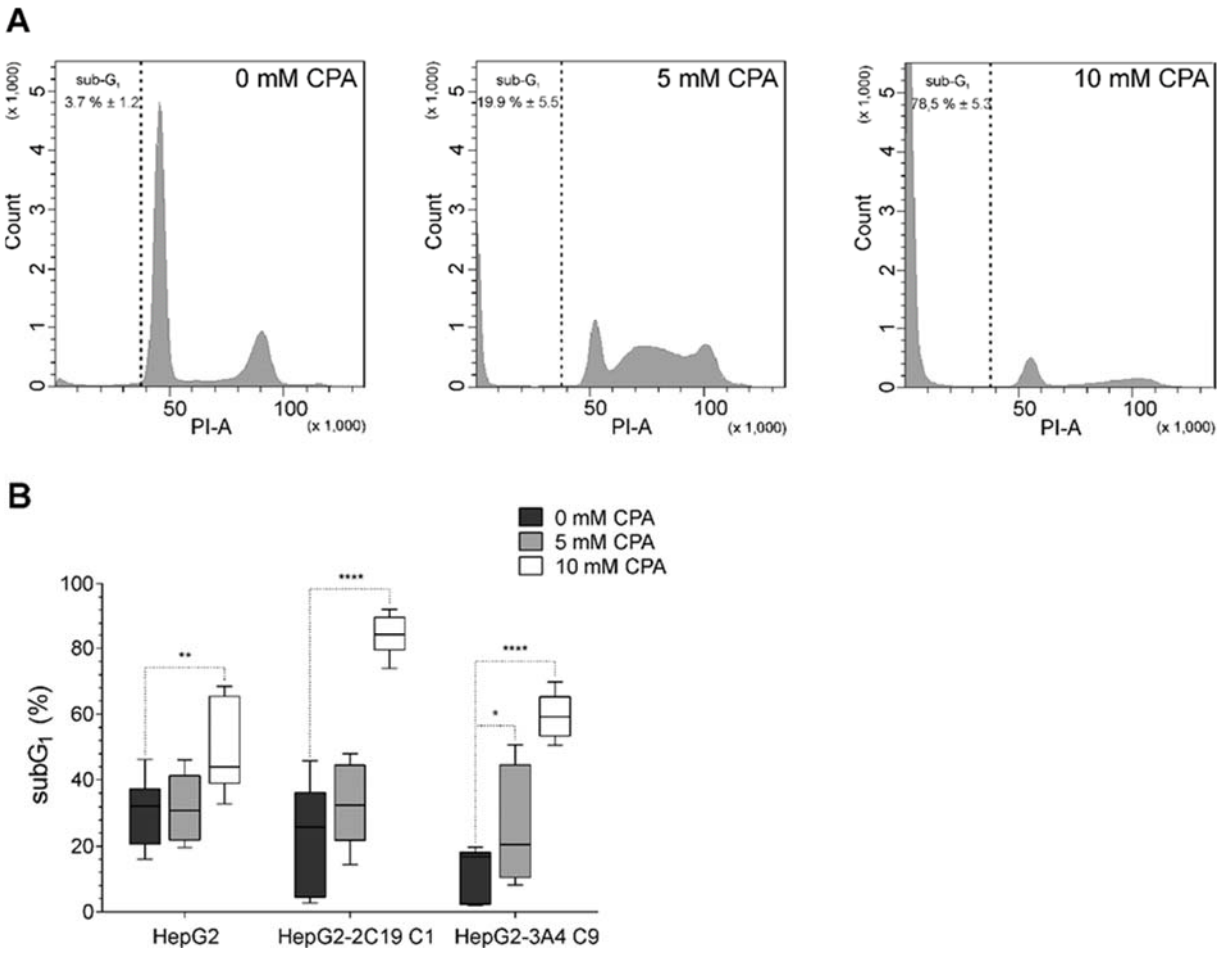

Fig. 6 CPA affects cell cycle progression. After ethanol fixation of CPA-treated cells and DNA staining by PI, cell cycle distribution was analyzed by flow cytometry. (**a**) Representative histograms with DNA contents (PI-A) of CPA-treated or untreated HepG2-2C19 C1 cells; (**b**) Quantification of dead (apoptotic) cells peaking at "sub-G_1". Boxplot: Whiskers represent 10th to 90th percentiles, horizontal lines within the box represent median values ± SD of sub-G_1; *p<0.05; **p<0.01; ****p<0.0001.

Altogether, we found marked differences of acute cytotoxic CPA effects between CYP2C19 and -3A4 overexpressing cell clones and their parental counterpart if biological endpoints such as cell membrane integrity, DNA damage and cell death formation were investigated. Apparently, analysis of only metabolic activity led to dramatic underestimation of acute CPA cytotoxicity.

4. Discussion

Acute or chronic drug-induced liver injuries (DILI) are major obstacles during clinical drug testing and upon market approval. In order to accurately predict cytotoxic effects *in vitro*,

numerous studies have been performed using *in vitro* cell cultures of hepatocytes. Besides primary human hepatocytes that unfortunately do not proliferate *in vitro*, human hepatoma cell line HepG2 has been intensively used in the past. Since their first description in 1979 (Aden et al. 1979), numerous studies showed that HepG2 cells retained important features of differentiated hepatocytes such as albumin secretion (Busso et al. 1990), glycogen synthesis (Meier et al. 2007) and conjugating (phase II) enzymes (Kade et al. 2016; Lamy et al. 2008). Moreover, HepG2 cells are still the most frequently used *in vitro* system for analyzing drug cytotoxicity, including metabolic activity assays based on reduction of tetrazolium dyes XTT, MTT and WTS or on ATP detection (Kamalian et al. 2015; Nowak et al. 2018; Rudzok et al. 2010; Xu et al. 2018). Since those cells lack physiologically relevant expression levels of most phase I enzymes, different groups aimed to improve the HepG2 cell system via transient or even stable overexpression of defined CYP450 enzymes (Frederick et al. 2011; Herzog et al. 2015; Hosomi et al. 2011; Tolosa et al. 2013; Yoshitomi et al. 2001).

Here, we present a new HepG2 cell clone stably overexpressing CYP2C19 (clone 1). Normalized to total protein amounts, intact cells from the clone displayed high enzymatic activity of CYP2C19, showing nearly the same conversion of model substrate tolbutamide as cryopreserved human liver microsomes. This was more than we expected since liver microsomes represent a subcellular fraction highly enriched for CYP enzymes. Since 4-hydroxytolbutamide is known to be formed by CYP2C9 and CYP2C19, the calculated microsomal activity represents the combined action of both CYP enzymes. However, CYP2C9 makes up between 15-20 % of total CYP protein and thus is, after CYP3A4, the second most abundant phase I enzyme while CYP2C19 contributes to not more than 5 % of CYP protein (Donato and Castell 2003). Based on inhibitory experiments with microsomal proteins, it was in fact shown that CYP2C19 makes up about 14-22 % of total tolbutamide hydroxylation activity (Wester et al. 2000). In general, CYP2C19 was found to display nearly identical turnover, kinetical and inhibitory characteristics as CYP2C9 (Lasker et al. 1998). Since there is almost no background CYP2C9 expression in HepG2 cells (Wilkening et al.

2003), we thus estimate the CYP2C19 catalytic activity of HepG2 cell clone 1 to be about five-fold higher than that of average human liver microsomes which were cryopreserved. It is well known that enzymatic activities of most CYPs significantly drop down upon pHH isolation, cryopreservation and *in vitro* culturing (Kammerer and Küpper 2018). Microsomes represent a subcellular fraction enriched for phase I enzymes. Since we found the CYP2C19 enzyme activity of our HepG2 cell clone exceeding that of cryopreserved microsomes, it is conceivable that it even approaches the physiological value of human hepatocytes within their natural tissue environment. Because of their high CYP enzyme activities and their phenotypic stability over many passages, both HepG2 cell clones (HepG2-2C19 C1 and HepG2-3A4 C9) seem to be promising as reference cell clones for benchmarking these phase I enzymes. Additionally, these cell-based systems should be helpful to investigate functions of CYP2C19 and CYP3A4 in the metabolism-dependent cytotoxicity of xenobiotics. Here we were interested to reassess the cytotoxic effect of common cytostatic cyclophosphamide (CPA).

CPA is known as a representative compound for bioactivation by CYP3A4 and -2C19 (Chang et al. 1993; Griskevicius et al. 2003; Ren et al. 1997; Roy et al. 1999). In this study, HepG2 cell clones expressing functional CYP3A4 and CYP2C19 generally showed higher sensitivity to CPA than parental HepG2 cells. However, when analyzing 10 mM CPA-induced cytotoxicity with metabolic assays such as XTT test or ATP assay, a reduction of more than 50 % of metabolic activity was never measured. Based on such assays, acute cytotoxicity of 10 mM CPA would be assessed to be only moderate. It has to be taken into account that according to a 1996 guideline of the International Conference on Harmonisation of Technical Requirements for Registration of Pharmaceuticals for Human Use (ICH), the top concentration of a pharmaceutical drug to be tested in mammalian cell cultures should not exceed 10 mM. More recently, ICH recommended reducing this concentration to 1 mM in order to avoid side effects due to increased osmolality. Furthermore, it has to be considered that the *in vitro* applied dose of 10 mM CPA is much higher than can be found in the plasma of cancer patients shortly after infusion with 1000

mg/m^2 CPA. Prior to infusion, CPA typically is reconstituted with normal saline to a concentration of 20 mg/ml (77 mM) CPA. Although the initial CPA concentration is thus much higher than we did use for our *in vitro* tests, it immediately drops down to plasma dilution. It was found that 1 hour after 1000 mg/m^2 CPA administration plasma levels were already at 20.5 μg/mL (0.08 mM) (Struck et al. 1987). In any case, to detect genotoxicity of a drug the top concentration should lead to at least 50 % cytotoxicity according to the guidelines. Since with 1 mM CPA there was almost no acute cytotoxicity detectable with ATP or XTT tests (data not shown), we decided to keep at 10 mM CPA as the highest concentration. This concentration for *in vitro* toxicity testing on HepG2 cells was also used by other groups (Choi et al. 2015; Donato et al. 2013). We thus think that for our cell system, 10 nM CPA is a relevant concentration to investigate acute cyto- and genotoxicity.

Most likely, CPA-mediated cytotoxicity is due to the formation of metabolites such as acrolein and PM. PM is thought to cause most of the CPA-mediated cytotoxicity along with the main metabolization pathway. However, it has to be noted that acrolein also contributes to cytotoxicity (Alarcon and Meienhofer 1971; Crook et al. 1986; Kehrer and Biswal 2000). Indeed, we could not only identify direct phase I metabolite 4-OH-CPA (Supplementary material, Fif. S2), but also its further procuct acrolein (Fig. 3) in CPA-treated HepG2 cell clone supernatants, but not in those of parental HepG2 cells. While the protein-binding compound acrolein was shown to cause ER stress and to interfere with mitochondrial integrity (Mohammad et al. 2012), PM is a bifunctional DNA-alkylating agent. Subsequently, CPA-mediated DNA damages such as intra- and interstrand DNA cross-links (Ganesan and Keating 2015; Schärer 2005) should lead to the formation of DNA double strand breaks. Such DNA breaks can be conventionally monitored by the formation of γH2AX foci which should correlate with the number of DNA double strand breaks (Kuo and Yang 2008; Plesca et al. 2008; Willitzki et al. 2013). We could demonstrate that CPA treatment led to dose-dependent γH2AX formation which provides strong evidence for PM-induced genotoxicity in HepG2 cells and clones derived thereof (Fig. 5). To the best of our knowledge, this is the first published report on genotoxicity detection by γH2AX formation in CPA-treated HepG2

cells. Remarkably, the extent of measured acute genotoxicity was in clear contrast to only moderate CPA effects on assays for metabolic activity: HepG2 clones treated with 5 or 10 mM CPA showed higher than 50-fold increases of nuclei containing accumulated γH2AX foci compared to non-treated cells while metabolic activity assays revealed only moderate decreases. It should be noted here that the moderate metabolic effect of CPA on HepG2 clones might have been superimposed by the so-called “Warburg effect”, i.e. using of lactate fermentation to produce energy versus oxidative phosphorylation (Kamalian et al. 2015; Vander Heiden and DeBerardinis 2017). However, those cytotoxicity assays like XTT measure the total cellular production of reduced pyridine nucleotides NADH/NADPH (Vistica et al. 1991) and not only mitochondrial activity. Therefore, they should also work in cells with Warburg effect, but might have lower sensitivity. Mechanistically, DNA double strand break formation by CPA, as visualized by γH2AX foci, and break down of reduced pyridine nucleotides, as measured by XTT assay, are not directly linked. The first event is DNA crosslinking by CPA metabolite PM. Subsequent formation of double strand breaks induce double strand break repair processes, i.e. non-homologous end joining or homologous recombination. Both lead to the formation of γH2AX foci (Feng et al. 2017; Scully and Xie 2013). Foci thus represent early events of DNA damage and repair. It was shown that the observed decay of γH2AX foci after ionizing radiation correlated with successful double strand break repair (Van Oorschot et al. 2014). We speculate that many DNA damages by CPA exposure will be repaired without causing any metabolic effect. By contrast, breakdown of pyridine nucleotides as measured by XTT might be a later cellular end-point. On the other hand, extraordinary high acute genotoxicity at 10 mM CPA is paralleled by dramatic decreases of cell membrane integrity as measured by trypan blue exclusion test (Fig. 4) and increases of cell death events (sub-G_1 cells) as measured with flow cytometry (Fig. 6). Furthermore, cell cycle analyses showed that CPA treatment led to an accumulation of S phase cells, which is in line with previous studies (Cai et al. 2001; Dean and Fox 1984).

Interestingly, overexpression of CYP2C19 apparently caused more DNA double strand break events at all tested CPA concentrations in comparison with CYP3A4 overexpression. This is consistent with a relatively higher conversion of CPA into 4-OH-CPA (Supplementary material, Fig. S2) and acrolein (Fig. 3) by CYP2C19-overexpressing HepG2 cells. By contrast, CPA treatment of CYP3A4-overexpressing HepG2 cells exerted stronger effects on cell membrane integrity (Fig. 4) and even on metabolic activity (Fig. 2) as is the case with CYP2C19 overexpression. In addition to monooxygenation reaction on CPA finally leading to pharmacologically active metabolite PM, CYP3A4 can also convert CPA into N-dechloroethylated metabolites (Huang et al. 2000). Employing this alternative pathway should lead to reduced formation of active metabolite PM resulting in reduced genotoxicity. This, in turn, should yield less γH2AX foci while alternative metabolization product 2-dechloroethyl cyclophosphamide (DECP) gives rise to chloroacetaldehyde (Yang et al. 2017), a well-known toxic agent. This might explain observed increases of some parameters of cytotoxicity in CPA-treated CYP3A4-overexpressing cells while genotoxicity apparently is less pronounced compared to CYP2C19 overexpression.

5. Conclusions

Each generated CYP-expressing HepG2 cell clone (HepG2-2C19 C1 and HepG2-3A4 C9) add to the well-known hepatic equipment of the parental cell line a reproducible, high-end activity of a certain CYP enzyme making these clones a relevant model for investigating functions of CYP2C19 and CYP3A4 in the metabolism-dependent cytotoxicity of xenobiotics. Additionally, it can be concluded that standard metabolic activity tests with XTT, MTT, MTS or on ATP levels could dramatically underestimate acute cytotoxic effects of CPA and probably other genotoxic compounds. Using the γH2AX foci test could be an additional option to avoid false negative results for *in vitro* cytotoxicity analysis.

Acknowledgments

This work was supported by the European Fonds of Regional Development (EFRE, Brandenburg, Germany; project “PERsonalisierte Medizin durch FUNCTIONomics in Berlin-Brandenburg: Drug-Metabolisierungsmodul für Wirkstofftests an Patientenzellen”; project number: 85002925); and the Ministry for Science, Research and Cultural Affairs of Brandenburg through the grant of the joint project “Konsequenzen der Alters-assoziierten Zell- und Organfunktion” of the Gesundheitscampus Brandenburg (project number: GeCa H228-05/002/008).

Conflict of interest

The authors declare that they have no conflicts of interest with the contents of this article.

References

Aden, D.P., Fogel, A., Plotkin, S., Damjanov, I. and Knowles, B.B., 1979. Controlled snthesis of HBsAg in a differentiated human liver carcinoma-derived cell line. Nature. 282, 615-616.

Alarcon, R. and Meienhofer, J., 1971. Formation of the cytotoxic aldehyde acrolein during in vitro degradation of cyclophosphamide. Nature. 233, 250-252.

Aninat C, Piton A, Glaise D, Le, C.T., Langouet, S., Morel, F. Guguen-Guillouzo, C. and Guillouzo, A., 2006. Expression of cytochromes P450, conjugating enzymes and nuclear receptors in human hepatoma HepaRG cells. Drug Metab Dispos 34, 75-83.

Belfayol L, Guillevin L, Louchahi K, Lortholary O, Bosio A and Fauvelle F, 1995. Measurement of 4-hydroxycyclophosphamide in serum by reversed-phase high-performance liquid chromatography. Journal of Chromatography B: Biomedical Sciences and Applications 663, 395-399.

Beneke R, Geisen C, Zevnik B, Bauch T, Muller WU, Kupper JH and Moroy T, 2000. DNA excision repair and DNA damage-induced apoptosis are linked to Poly(ADP-ribosyl)ation but have different requirements for p53. Mol Cell Biol. 20, 6695-6703.

Burkard A, Dähn C, Heinz S,Zutavern A, Sonntag-Buck V, Maltman D, Przyborski S, Hewitt NJ and Braspenning J, 2012. Generation of proliferating human hepatocytes using upcyte((R)) technology: characterisation and applications in induction and cytotoxicity assays. Xenobiotica. 42, 939-956.

Busso, N., Chesne, C., Delers, F., Morel, F. and Guillouzo, A., 1990. Trensforming growth-factor-beta (TGF-beta) inhibits albumin synthesis in normal human hepatocytes and in hepatoma HepG2 cells. Biochem Biophys Res Commun. 171, 647-654.

Cai Y, Ludeman SM, Wilson LR, Chung AB and Dolan ME, 2001. Effect of O6-Benzylguanine on Nitrogen Mustard-induced Toxicity, Apoptosis, and Mutagenicity in Chinese Hamster Ovary Cells. Molecular Cancer Therapeutics 1, 21-28.

Castell JV, Jover R, Martnez-Jimnez CP and Gmez-Lechn MJ, 2006. Hepatocyte cell lines: their use, scope and limitations in drug metabolism studies. Expert Opinion on Drug Metabolism & Toxicology 2, 183-212.

Chan R and Benet LZ, 2017. Evaluation of DILI Predictive Hypotheses in Early Drug Development. Chem Res Toxicol 30, 1017-1029.

Chang TK, Yu L, Goldstein JA and Waxman DJ, 1997a. Identification of the polymorphically expressed CYP2C19 and the wild-type CYP2C9-ILE^{359} allele as low-K_m catalysts of cyclophosphamide and ifosfamide activation. Pharmacogenetics and Genomics 7, 211-221.

Chang TKH, Weber GF, Crespi CL and Waxman DJ, 1993. Differential Activation of Cyclophosphamide and Ifosphamide by Cytochromes P-450 2B and 3A in Human Liver Microsomes. Cancer Research. 53, 5629-5637.

Chang TKH, Yu L, Maurel P and Waxman DJ, 1997b. Enhanced Cyclophosphamide and Ifosfamide Activation in Primary Human Hepatocyte Cultures: Response to Cytochrome P-450 Inducers and Autoinduction by Oxazaphosphorines. Cancer Research 57, 1946-1954.

Chernoff N, Rogers JM, Alles AJ, Zucker RM, Elstein KH, Massaro EJ and Sulik KK, 1989. Cell cycle alterations and cell death in cyclophosphamide teratogenesis. Teratog Carcinog Mutagen. 9, 199-209.

Choi JM, Oh SJ, Lee J-Y, Jeon JS, Ryu CS, Kim Y-M, Lee K and Kim SK, 2015. Prediction of Drug-Induced Liver Injury in HepG2 Cells Cultured with Human Liver Microsomes. Chemical Research in Toxicology. 28, 872-885.

Colvin M, Brundrett RB, Kan M-NN, Jardine I and Fenselau C, 1976. Alkylating Properties of Phosphoramide Mustard. Cancer Research. 36, 1121-1126.

Crook TR, Souhami RL and McLean AEM, 1986. Cytotoxicity, DNA Cross-Linking, and Single Strand Breaks Induced by Activated Cyclophosphamide and Acrolein in Human Leukemia Cells. Cancer Research. 46, 5029-5034.

Darzynkiewicz Z, Halicka HD and Zhao H, 2010. Analysis of Cellular DNA Content by Flow and Laser Scanning Cytometry. Advances in experimental medicine and biology. 676, 137-147.

Dean SW and Fox M, 1984. DNA repair, DNA synthesis and cell cycle delay in human lymphoblastoid cells differentially sensitive to the cytotoxic effects of nitrogen mustard. Mutation Research/DNA Repair Reports. 132, 63-72.

Donato MT and Castell JV, 2003. Strategies and molecular probes to investigate the role of cytochrome P450 in drug metabolism: focus on in vitro studies. Clin Pharmacokinet. 42, 153-78.

Donato MT, Ramiro J and Gomez-Lechón MJ, 2013. Hepatic Cell Lines for Drug Hepatotoxicity Testing: Limitations and Strategies to Upgrade ther Metabolic Competence by Gene Engineering. Current Drug Metabolism. 14, 946-968.

Feng YL, Xiang JF, Liu SC, Guo T, Yan GF, Feng Y, Kong N, Li HD, Huang Y, Lin H, Cai XJ and Xie AY, 2017. H2AX facilitates classical non-homologous end joining at the expense of limited nucleotide loss at repair junctions. Nucleic Acids Res. 45, 10614-10633.

Fleming RA, 1997. An overview of cyclophosphamide and ifosfamide pharmacology. Pharmacotherapy 17, 146S-154S.

Frederick DM, Jacinto EY, Patel NN, Rushmore TH, Tchao R and Harvison PJ, 2011. Cytotoxicity of 3-(3,5-dichlorophenyl)-2,4-thiazolidinedione (DCPT) and analogues in wild type and CYP3A4 stably transfected HepG2 cells. Toxicology in Vitro 25, 2113-2119.

Ganesan S and Keating AF, 2015. Phosphoramide mustard exposure induces DNA adduct formation and the DNA damage repair response in rat ovarian granulosa cells. Toxicology and Applied Pharmacology 282, 252-258.

Gerets HHJ, Tilmant K, Gerin B, Chanteux H, Depelchin BO, Dhalluin S and Atienzar FA, 2012. Characterization of primary human hepatocytes, HepG2 cells, and HepaRG cells at the mRNA level and CYP activity in response to inducers and their predictivity for the detection of human hepatotoxins. Cell Biology and Toxicology 28, 69-87.

Ghallab A, 2014. The rediscovery of HepG2 cells for prediction of drug induced liver injury (DILI). EXCLI J 13, 1286-1288.

Griskevicius L, Yasar Ü, Sandberg M,Hidestrand, M, Eliasson E, Tybring G, Hassan M and Dahl M-L, 2003. Bioactivation of cyclophosphamide: the role of polymorphic CYP2C enzymes. European Journal of Clinical Pharmacology 59, 103-109.

Guillouzo A, Corlu A, Aninat C, Glaise D, Morel F, Guguen-Guillouzo C, 2007. The human hepatoma HepaRG cells: a highly differentiated model for studies of liver metabolism and toxicity of xenobiotics. Chem Biol Interact. 168, 66-73.

Herzog N, Hansen M, Miethbauer S, Schmidtke KU, Anderer U, Lupp A, Sperling S, Seehofer D, Damm G, Scheibner K and Küpper J-H, 2016. Primary-like human hepatocytes genetically engineered to obtain proliferation competence display hepatic differentiation characteristics in monolayer and organotypical spheroid cultures. Cell Biol Int. 40,341-353.

Herzog N, Katzenberger N, Martin F, Schmidtke K-U, Küpper J-H, 2015. Generation of cytochrome P450 3A4-overexpressing HepG2 cell clones for standardization of hepatocellular testosterone 6β-hydroxylation activity. Journal of Cellular Biotechnology. 1, 15-26.

Hohorst H-J, Peter G, Struck RF, 1976. Synthesis of 4-Hydroperoxy Derivatives of Ifosfamide and Trofosfamide by Direct Ozonation and Preliminary Antitumor Evaluation in Vivo. Cancer Research 36, 2278-2281.

Hosomi H, Fukami T, Iwamura A, Nakajima M and Yokoi T, 2011. Development of a Highly Sensitive Cytotoxicity Assay System for CYP3A4-Mediated Metabolic Activation. Drug Metabolism and Disposition 39, 1388-1395.

Huang Z, Roy P and Waxman DJ, 2000. Role of human liver microsomal CYP3A4 and CYP2B6 in catalyzing N-dechloroethylation of cyclophosphamide and ifosfamide. Biochem Pharmacol 59, 961-972.

Kade S, Herzog N, Schmidtke K-U and Küpper J-H, 2016. Chronic ethanol treatment depletes glutathione regeneration capacity in hepatoma cell line HepG2. Journal of Cellular Biotechnology. 1, 13.

Kamalian L, Chadwick AE, Bayliss M, French NS, Monshouwer M, Snoeys J and Park BK, 2015. The utility of HepG2 cells to identify direct mitochondrial dysfunction in The absence of cell death. Toxicol In Vitro. 29, 732-740.

Kammerer S and Küpper J-H, 2018. Human hepatocyte systems for in vitro toxicology analysis. Journal of Cellular Biotechnology. 3, 85-93.

Kanebratt KP and Andersson TB, 2008. Evaluation of HepaRG cells as an in vitro model for human drug metabolism studies. Drug Metab Dispos 36, 1444-1452.

Kehrer JP and Biswal SS, 2000. The Molecular Effects of Acrolein. Toxicological Sciences. 57, 6-15.

Kuo LJ and Yang L-X, 2008. γ-H2AX-a novel biomarker for DNA double-strand breaks. In vivo 22, 305-309.

Lamy E, Volkel Y, Roos PH, Kassie F and Mersch-Sundermann V, 2008. Ethanol enhanced the genotoxicity of acrylamide in human, metabolically competent HepG2 cells by CYP2E1 induction and glutathione depletion. Int J Hyg Environ Health. 211, 74-81.

Lasker JM, Wester MR, Aramsombatdee E and Raucy JL, 1998. Characterization of CYP2C19 and CYP2C9 from Human Liver: Respective Roles in Microsomal Tolbutamide, S-Mephenytoin, and Omeprazole Hydroxylations. Archives of Biochemistry and Biophysics 353, 16-28.

Levy G, Bomze D, Heinz S, Ramachandran SD, Noerenberg A, Cohen M, Shibolet O, Sklan E, Braspenning J and Nahmias Y, 2015. Long-term culture and expansion of primary human hepatocytes. Nat Biotechnol 33, 1264-1271.

Li W, Zhou J and Xu Y, 2015. Study of the in vitro cytotoxicity testing of medical devices. Biomed Rep. 3, 617-620.

Low JE, Borch RF and Sladek NE, 1982. Conversion of 4-Hydroperoxycyclophosphamide and 4-Hydroxycyclophosphamide to Phosphoramide Mustard and Acrolein Mediated by Bifunctional Catalysts. Cancer Research 42, 830-837.

Lubberstedt M, Muller-Vieira U, Mayer M, Biemel KM, Knospel F, Knobeloch D, Nussler AK, Gerlach JC and Zeilinger K, 2011. HepaRG human hepatic cell line utility as a surrogate for primary human hepatocytes in drug metabolism assessment in vitro. J Pharmacol Toxicol Methods. 63, 59-68.

Meier M, Klein HH, Kramer J, Drenckhan M and Schutt M, 2007. Calpain inhibition impairs glycogen synthesis in HepG2 hepatoma cells without altering insulin signaling. J Endocrinol. 193, 45-51.

Mohammad MK, Avila D, Zhang J, Barve S, Arteel G, McClain C and Joshi-Barve S, 2012. Acrolein cytotoxicity in hepatocytes involves endoplasmic reticulum stress, mitochondrial dysfunction and oxidative stress. Toxicol Appl Pharmacol. 265, 73-82.

Nowak E, Kammerer S and Küpper J-H, 2018. ATP-based cell viability assay is superior to trypan blue exclusion and XTT assay in measuring cytotoxicity of anticancer drugs Taxol and Imatinib, and proteasome inhibitor MG-132 on human hepatoma cell line HepG2. Clin Hemorheol Microcirc. 69, 327-336.

Plesca D, Mazumder S and Almasan A, 2008. DNA Damage Response and Apoptosis. Methods in enzymology. 446, 107-122.

Ren S, Yang J-S, Kalhorn TF and Slattery JT, 1997. Oxidation of Cyclophosphamide to 4-Hydroxycyclophosphamide and Deschloroethylcyclophosphamide in Human Liver Microsomes. Cancer Research. 57, 4229-4235.

Riss TL, Moravec RA, Niles AL, Duellman S, Benink HA, Worzella TJ and Minor L, 2004. Cell Viability Assaya. In: G.S. Sittampalam, N.P. Coussens, K. Brimacombe, A. Grossman, M. Arkin, D. Auld, C. Austin, J. Baell, B. Bejcek, T.D.Y. Chung, J.L. Dahlin, V. Devanaryan, T.L. Foley, M. Glicksman, M.D. Hall, J.V. Hass, J. Inglese, P.W. Iversen, S.D. Kahl, S.C. Kales, M. Lal-Nag, Z. Li, J. McGee, O. McManus, T. Riss, O.J. Trask, Jr., J.R. Weidner, M. Xia and X. Xu (Eds,), Assay Guidance Manual, Bethesda (MD).

Rodríguez-Antona C, Donato MT, Boobis A, Edwards RJ, Watts PS, Castell JV and Gomez-Lechón MJ, 2002. Cytochrome P450 expression in human hepatocytes and hepatoma cell lines: molecular mechanisms that determine lower expression in cultured cells. Xenobiotica 32, 505-520.

Rodriguez-Antona C and Ingelman-Sundberg M, 2006. Cytochrome P450 pharmacogenetics and cancer. Oncogene 25, 1679-1691.

Roy P, Yu LJ, Crespi CL and Waxman DJ, 1999. Development of a Substrate-Activity Based Approach To Identify the Major Human Liver P-450 Catalysts of Cyclophosphamide and Ifosfamide Activation Based on cDNA-Expressed Activities and Liver Microsomal P-450 Profiles. Drug Metabolism and Disposition 27, 655-666.

Rudzok S, Schlink U, Herbarth O and Bauer M, 2010. Measuring and modeling of binary mixture effects of pharmaceuticals and nickel on cell viability/cytotoxicity in the human hepatoma derived cell line HepG2. Toxicol Appl Pharmacol. 244, 336-343.

Rueff J, Chiapella C, Chipman JK, Darroudi F, Duarte Silva I, Duverger-van Bogaert M, Fonti E, Glatt HR, Isern P, Laires A, Leonard A. Llagostera M, Mossesso P, Natarajan AT, Palitti F, Rodrigues AS, Schinoppi A, Turchi G and Werle-Schneider G, 1996. Development and validation of alternative metabolic systems for mutagenicity testing in short-term assays. Mutation Research/Fundamental and Molecular Mechanisms of Mutagenesis 353, 151-176.

Schärer OD, 2005. DNA Interstrand Crosslinks: Natural and Drug-Induced DNA Adducts that Induce Unique Cellular Responses. ChemBioChem 6, 27-32.

Scully R and Xie A, 2013. Double strand break repair functions of histone H2AX. Mutat Res. 750, 5-14.

Sladek NE, 1988. Metabolism of oxazaphosphorines. Pharmacology & Therapeutics 37, 301-355.

Stepanenko AA and Dmitrenko VV, 2015. Pitfalls of the MTT assay: Direct and off-target effects of inhibitors can result in over/underestimation of cell viability. Gene. 574, 193-203.

Struck RF, Alberts DS, Horne K, Phillips JG, Peng YM and Roe DJ, 1987. Plasma pharmacokinetics of cyclophosphamide and its cytotoxic metabolites after intravenous versus oral administration in a randomized, crossover trial. Cancer Res. 47, 2723-2726.

Sumantran VN, 2011. Cellular chemosensitivity assays: an overview. Methods Mol Biol. 731, 219-236.

Tolosa L, Gómez-Lechón MJ, Pérez-Cataldo G, Castell JV and Donato MT, 2013. HepG2 cells simultaneously expressing five P450 enzymes for the screening of hepatotoxicity: identification of bioactivable drugs and the potential mechanism of toxicity involved. Archives of Toxicology 87, 1115-1127.

Van Oorschot B, Oei AL, Nuijens AC, Rodermond H, Hoeben R. Stap J, Stalpers LJ and Franken NA, 2014. Decay of gamma-H2AX foci correlates with potentially lethal damage repair and P53 status in human colorectal carcinoma cells. Cell Mol Biol Lett. 19, 37-51.

Vander Heiden MG and DeBerardinis RJ, 2017. Understanding the Intersections between Metabolism and Cancer Biology. Cell 168, 657-669.

Vellonen KS, Honkakoski P and Urtti A, 2004. Substrates and inhibitors of efflux proteins interfere with the MTT assay in cells and may lead to underestimation of drug toxicity. Eur J Pharm Sci. 23, 181-188.

Vistica DT, Skehan P, Scudiero D, Monks A, Pittman A and Boyd MR, 1991. Tetrazolium-based assays for cellular viability: a critical examination of selected parameters affecting formazan production. Cancer Res. 51, 2515-2520.

Wang P, Henning SM and Heber D, 2010. Limitations of MTT and MTS-based assays for measurement of antiproliferative activity of green tea polyphenols. PLoS One. 5, e10202.

Wester MR, Lasker JM, Johnson EF and Raucy JL, 2000. CYP2C19 Participates in Tolbutamide Hydroxylation by Human Liver Microsomes. Drug Metabolism and Disposition 28, 354-359.

Westerink WMA and Schoonen WGEJ, 2007. Cytochrome P450 enzyme levels in HepG2 cells and cryopreserved primary human hepatocytes and their induction in HepG2 cells. Toxicology in Vitro 21, 1581-1591.

Wilkening S, Stahl F and Bader A, 2003. Comparison of primary human hepatocytes and hepatoma cell line HepG2 with regard to their biotransformation properties. Drug Metabolism and Disposition 31, 1035-1042.

Willitzki A, Lorenz S, Hiemann R,Guttek K, Goihl A, Hartig R, Conrad K, Feist E, Sack U, Schierack P, Heiserich L, Eberle C, Peters V, Roggenbuck D and Reinhold D, 2013. Fully automated analysis of chemically induced gammaH2AX foci in human peripheral blood mononuclear cells by indirect immunofluorescence. Cytometry A. 83, 1017-1026.

Xu J, Oda S and Yokoi T, 2018. Cell-based assay using glutathione-depleted HepaRG and HepG2 human liver cells for predicting drug-unduced liver injury. Toxicol In Vitro. 48, 286-301.

Yang L, Yan C, Zhang F, Jiang B, Gao S, Liang Y, Huang L and Chen W, 2018. Effects of ketoconazole on cyclophosphamide metabolism: evaluation of CYP3A4 inhibition effect using the in vitro and in vivo models. Exp Anim. 67, 71-82.

Yoshitomi S, Ikemoto K, Takahashi J, Miki H, Namba M and Asahi S, 2001. Establishment of the transformants expressing human cytochrome P450 subtypes in HepG2, and their applications on drug metabolism and toxicology. Toxicology in Vitro 15, 245-256.

Zhou C, Li Z, Diao H, Yu Y, Zhu W, Dai Y, Chen FF and Yang J, 2006. DNA damage evaluated by γH2AX foci formation by a selective group of chemical/physical stressors. Mutation research 604, 8-18.